

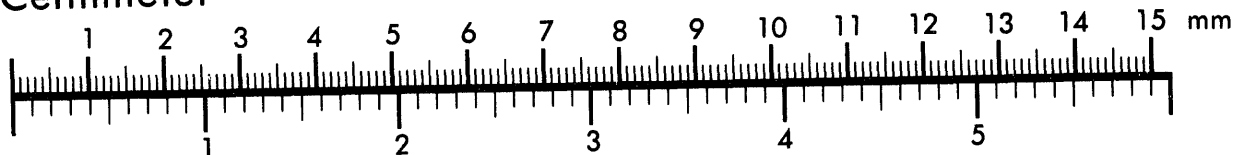


## AIM

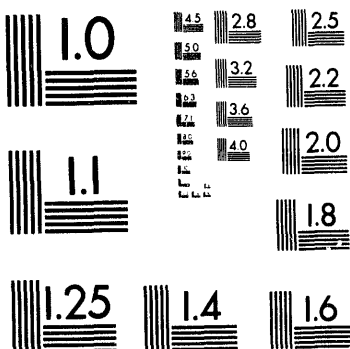
Association for Information and Image Management

1100 Wayne Avenue, Suite 1100  
Silver Spring, Maryland 20910  
301/587-8202

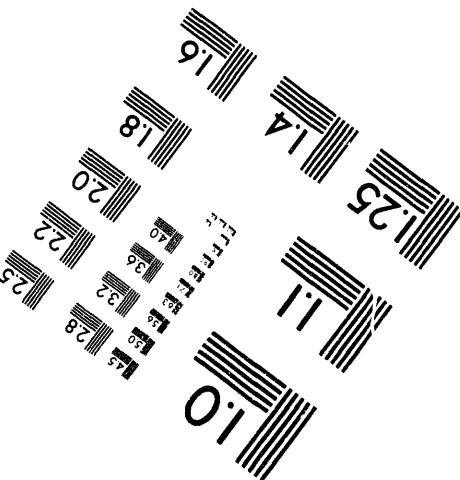
## Centimeter



## Inches



MANUFACTURED TO AIIM STANDARDS  
BY APPLIED IMAGE, INC.



1 of 1

# AN ADAPTIVE PROJECTION METHOD FOR THE INCOMPRESSIBLE NAVIER-STOKES EQUATIONS

*Ann S. Almgren, John B. Bell, Louis H. Howell \**  
Lawrence Livermore National Laboratory, Livermore, CA 94550

*Phillip Colella †*  
University of California at Berkeley, Berkeley, CA 94720

## Abstract

In this paper we present a method for solving the time-dependent incompressible Navier-Stokes equations on an adaptive grid. The method is based on a projection formulation in which we first solve convection-diffusion equations to predict intermediate velocities, and then project these velocities onto a space of approximately divergence-free vector fields. Our treatment of convection uses a specialized second-order upwind method for differencing the nonlinear convection terms that provides a robust treatment of these terms suitable for high Reynolds number flows.

Our approach to adaptive refinement uses a nested hierarchy of grids with simultaneous refinement of the grids in both space and time. The integration algorithm on the grid hierarchy is a recursive procedure in which coarse grids are advanced, fine grids are advanced multiple steps to reach the same time as the coarse grids, and the grid levels are then synchronized.

## Introduction

The equations governing variable density incompressible flow can be written:

$$U_t + (U \cdot \nabla)U = -\frac{1}{\rho} \nabla p + LU + F, \quad (1.1)$$

$$\rho_t + (U \cdot \nabla)\rho = 0, \quad (1.2)$$

$$\nabla \cdot U = 0 \quad (1.3)$$

where  $U$ ,  $\rho$ , and  $p$  represent the velocity, density, and pressure, respectively,  $L$  is the operator representing the viscous forces (see [4]), and  $F$  represents any external forces. In this paper we develop a local adaptive mesh refinement algorithm for solving these equations, based on a second-order accurate projection method. The development of the single grid projection methodology for the incompressible Navier Stokes equations is discussed in [3] and [1]. The method presented here is an adaptive version of the algorithm in [1], generalized to include finite amplitude density variation as discussed in [4].

The focus of this paper is on incorporating a local adaptive mesh refinement algorithm (AMR) into the basic projection methodology. This algorithm uses a hierarchical grid approach first developed by Berger and Oliger [6]

\*This work of these authors was performed under the auspices of the U.S. Department of Energy by the Lawrence Livermore National Laboratory under contract W-7405-Eng-48. Support under contract W-7405-Eng-48 was provided by the AMS and HPCC Programs of the DOE Office of Scientific Computing and by the Defense Nuclear Agency under LACRO 93-817.

†Research supported at UC Berkeley by DARPA and the National Science Foundation under grant DMS-8919074; by a National Science Foundation Presidential Young Investigator award under grant ACS-8958522; and by the Department of Energy High Performance Computing and Communications Program under grant DE-FGO3-92ER25140.

MASTER  
DISTRIBUTION OF THIS DOCUMENT IS UNLIMITED

for hyperbolic partial differential equations, and demonstrated to be highly successful for high speed flow both in two [5] and three dimensions [2]. AMR is based on a sequence of nested grids with successively finer spacing in both time and space. New fine grids are created recursively until the solution is sufficiently resolved. Automated grid generation procedures dynamically create or remove rectangular fine grid patches as resolution requirements change.

### Single Grid Projection Algorithm

In this section we review the basic fractional step scheme for the case of a single uniform grid. The reader is referred to [1] and [3] for a more detailed description. The algorithm uses a staggered grid scheme in which velocity and density are given at cell centers and are denoted by  $U_{ij}^n$  and  $\rho_{ij}^n$  respectively. Pressure is specified at cell corners and is staggered in time, and is thus denoted by  $p_{i+\frac{1}{2}, j+\frac{1}{2}}^{n+\frac{1}{2}}$ .

The single grid algorithm for solving the system (1.1)-(1.3) is a fractional step scheme having two parts. First, we solve the advection-diffusion equations (1.1)-(1.2) for the updated density and an intermediate velocity field without strictly enforcing the incompressibility constraint. Then, we project this intermediate field onto the space of (approximately) discretely divergence-free vector fields.

For the advection-diffusion step we solve

$$\frac{\rho^{n+1} - \rho^n}{\Delta t} + [(U \cdot \nabla) \rho]^{n+\frac{1}{2}} = 0 \quad (2.1)$$

and

$$\frac{U^* - U^n}{\Delta t} + [(U \cdot \nabla) U]^{n+\frac{1}{2}} = -\frac{1}{\rho^{n+\frac{1}{2}}} \nabla p^{n-\frac{1}{2}} + L \frac{(U^* + U^n)}{2} + F \quad (2.2)$$

for the intermediate velocity  $U^*$  and the updated density  $\rho^{n+1}$ . The method uses an unsplit second-order upwind predictor-corrector scheme for evaluating the advective derivatives in (2.1)-(2.2). For this step the pressure gradient is evaluated at  $t^{n-\frac{1}{2}}$  and is treated as a source term in (2.2), with  $\rho^{n+\frac{1}{2}} = \frac{1}{2}(\rho^n + \rho^{n+1})$ . The predictor is described in more detail in [3], with transverse derivatives and slopes as in [1] and the extension to variable density as in [4]. The Crank-Nicholson discretization of the viscous terms requires solution of an elliptic equation for each velocity component; we use a standard five-point stencil for the Laplacian, and solve the resulting system using multigrid.

The velocity field  $U^*$  computed in the first step is not, in general, divergence-free. The projection step enforces the incompressibility constraint. A vector field decomposition is applied to  $\frac{U^* - U^n}{\Delta t}$  to obtain the new velocity field and an update for the pressure. In particular, if  $\mathbf{P}$  represents the projection then

$$\frac{U^{n+1} - U^n}{\Delta t} = \mathbf{P} \left( \frac{U^* - U^n}{\Delta t} \right) = \frac{U^* - U^n}{\Delta t} - \frac{1}{\rho^{n+\frac{1}{2}}} G\phi \quad (2.3)$$

$$\frac{1}{\rho^{n+\frac{1}{2}}} Gp^{n+\frac{1}{2}} = \frac{1}{\rho^{n+\frac{1}{2}}} Gp^{n-\frac{1}{2}} + (\mathbf{I} - \mathbf{P}) \left( \frac{U^* - U^n}{\Delta t} \right) = \frac{1}{\rho^{n+\frac{1}{2}}} (Gp^{n-\frac{1}{2}} + G\phi)$$

where  $\phi$  is found by solving a second-order accurate approximation to the equation

$$D \frac{1}{\rho} G\phi = D \left( \frac{U^* - U^n}{\Delta t} \right).$$

Here  $D$  and  $G$  are the discrete divergence and gradient operator, respectively. The elliptic equation which defines the projection is discretized using a standard nine-point finite difference method analogous to the finite element method with bilinear basis elements. We note that this is not a discrete orthogonal projection; in fact,  $DU^{n+1} \neq 0$ . However, the incompressibility constraint is approximated to second-order accuracy and the overall algorithm is stable. The reader is referred to [1] for a detailed discussion of this approximation to the projection.

The time-step restriction for the advective scheme is used to set the time step for the overall algorithm; this is set by the CFL condition:

$$\max_{ij} \left( \frac{|u_{ij}| \Delta t}{\Delta x}, \frac{|v_{ij}| \Delta t}{\Delta y} \right) = \sigma \leq 1,$$

## Adaptive Mesh Refinement

The initial creation of the grid hierarchy and the subsequent regridding operations in which the grids are dynamically changed to reflect changing flow conditions use the same procedures as were used in [2] for the hyperbolic case, with the exception of the error estimation procedure. The grid hierarchy is constructed using a simple error estimation criterion to determine where additional resolution is required; this criterion is determined by the user, and is typically the magnitude of vorticity, density, or density gradient. A proper nesting requirement is imposed at this stage, namely that the union of level  $\ell + 1$  grids be properly contained within the union of level  $\ell$  grids (except at the boundary of the physical domain where all levels can be refined up to the edge). This ensures that all coarse-fine interfaces are between successive levels; a level  $\ell + 2$  grid never directly interacts with a level  $\ell$  grid.

The procedure to advance level  $\ell$  one time step  $\Delta t^\ell$  is described below. The full algorithm is recursive, hence a full coarse grid time step is achieved by following this procedure for  $\ell = 0$ .

**Step 1.** For each grid at level  $\ell$  apply the upwind advection scheme to compute the nonlinear advective terms, and construct  $LU^n$ . For this calculation on each grid, data are provided on the grid to be integrated as well as on a border of cells sufficiently wide to advance the solution. Data are copied from other level  $\ell$  grids wherever such data are available; otherwise, data interpolated in space and time from coarser grids are used.

**Step 2.** If the flow is inviscid, add the advective terms, pressure term, and external source term to  $U^n$  on a grid-by-grid basis to construct  $U^{\ell,*}$  at  $t^\ell + \Delta t^\ell$ . If the flow is viscous, then solve the elliptic equation for  $U^{\ell,*}$  on all grids at level  $\ell$  simultaneously.

**Step 3.** Project  $U^{\ell,*}$  onto its (approximately) divergence-free part to obtain an initial approximation to  $U^\ell$  at  $t^\ell + \Delta t^\ell$ , by solving an equation analogous to (2.3). Dirichlet boundary conditions for  $\phi$  in the elliptic solve are interpolated from the level  $\ell - 1$  grids. We refer to this projection as a *level projection*, because it is used to update the velocities and pressure on all the grids at a single level; the data at every other level remains unchanged after a level projection. By itself, this projection is not sufficient to account properly for the coupling between levels in the elliptic equation defining the projection, inasmuch as it only forces matching of Dirichlet data at the coarse-fine interface, rather than both Dirichlet and Neumann data. The mismatch is corrected in Step 5 by a second type of projection.

**Step 4.** If there are grids at level  $\ell + 1$ , call the integration step recursively to advance the level  $\ell + 1$  grids. After the level  $\ell + 1$  grids complete  $r_\ell$  consecutive time steps, where  $r_\ell$  is the refinement ratio, typically two or four, the velocity and density data for all levels greater than or equal to  $\ell$  have been advanced to time  $t^\ell + \Delta t^\ell$ .

**Step 5.** If there are grids at level  $\ell + 1$ , use a *sync projection* to enforce the divergence constraint on the coarse-fine interface between levels  $\ell$  and  $\ell + 1$ . The divergence operator used to define the right-hand-side for the projection is defined at each node as an integral over adjacent cells; hence on the interface the divergence operates on data from both the coarse and fine levels. The sync projection correcting the mismatch between levels  $\ell$  and  $\ell + 1$  is used to adjust the velocities and pressure at both levels. The corrections are then interpolated up to grids at levels  $\ell + 2$  or greater, if they exist.

The linear system associated with the sync projection is the standard bilinear finite element stiffness matrix for a self-adjoint second-order elliptic operator. We solve this system using standard multigrid methods modified for use within the adaptive grid hierarchy. The multigrid algorithm for the level projection is straightforward since it only involves grids at a single level.

## Computational Results

In Figures 1 and 2 we show results from two different calculations using the adaptive projection method. The first (Figure 1) is an inviscid co-flowing jet, perturbed slightly at  $t = 0$  to break the symmetry. The boundary conditions are reflecting wall on top and bottom, inflow-outflow on left and right. The vorticity at time steps 290 and 291 is shown, with the level 1 grids at each time superimposed. The base grid is 128x256; the refinement ratio is four.

The second calculation (Figure 2) is of a variable density inviscid fluid swirling in a closed box. The initial conditions are:  $u(x, t = 0) = -\sin(2\pi y) \sin^2(\pi x)$ ,  $v(x, t = 0) = \sin(2\pi x) \sin^2(\pi y)$ ,

$$\rho(x, t = 0) = \begin{cases} 5. & \text{if } |x - (.25, .5)| < .2 \\ 1. & \text{otherwise} \end{cases}$$

in the unit square. The density at the 400th time step is shown, with the level 1 and level 2 grids superimposed. (The level 1 grids are drawn in black and the level 2 grids in white; the base grid is 96x96 and the refinement ratios are two and four for levels 1 and 2, respectively.)

The timings for the variable density problem indicate that the calculation took approximately 16  $\mu$ -seconds per cell advanced on one processor of a Cray C-90.

### Conclusions

We have developed a new adaptive projection method for time-dependent incompressible variable density flow. The levels in the adaptive mesh hierarchy are refined in both space and time. The advection step takes place on individual grids in an approach similar to that of the single grid method. The viscous solve and the projection at each level are similar to those in the single grid method, but must now incorporate multiple grids per level. In addition, we introduce a sync projection, which is needed to synchronize the solution at each level  $\ell$  with the data at the levels above it at the end of each level  $\ell$  time step. This adaptive projection method is second-order accurate and provides an efficient tool for modeling variable density flows.

### References

- [1] A. S. Almgren, J. B. Bell, and W. G. Szymczak. A numerical method for the incompressible Navier-Stokes equations based on an approximate projection. Technical Report UCRL-JC-112842, LLNL, January 1993.
- [2] J. B. Bell, M. J. Berger, J. S. Saltzman, and M. Welcome. Three dimensional adaptive mesh refinement for hyperbolic conservation laws. Technical Report UCRL-JC-108794, LLNL, Dec. 1991.
- [3] J. B. Bell, P. Colella, and H. M. Glaz. A second-order projection method for the incompressible Navier-Stokes equations. *J. Comput. Phys.*, 85:257–283, December 1989.
- [4] J. B. Bell and D. L. Marcus. A second-order projection method for variable-density flows. *J. Comput. Phys.*, 101:334–348, 1992.
- [5] M. J. Berger and P. Colella. Local adaptive mesh refinement for shock hydrodynamics. *J. Comput. Phys.*, 82:64–84, 1989.
- [6] M. J. Berger and J. Oliger. Adaptive mesh refinement for hyperbolic partial differential equations. *J. Comput. Phys.*, 53:484–512, 1984.

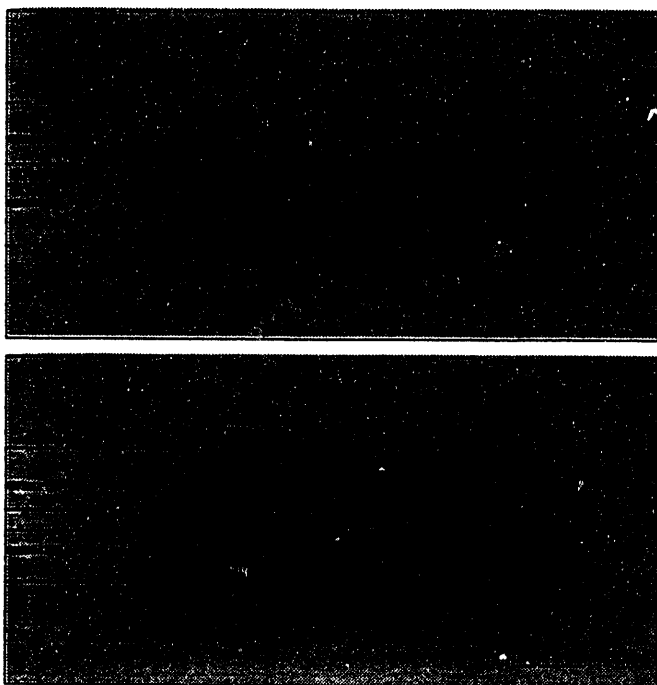


Figure 1. Vorticity and grids at level 1.

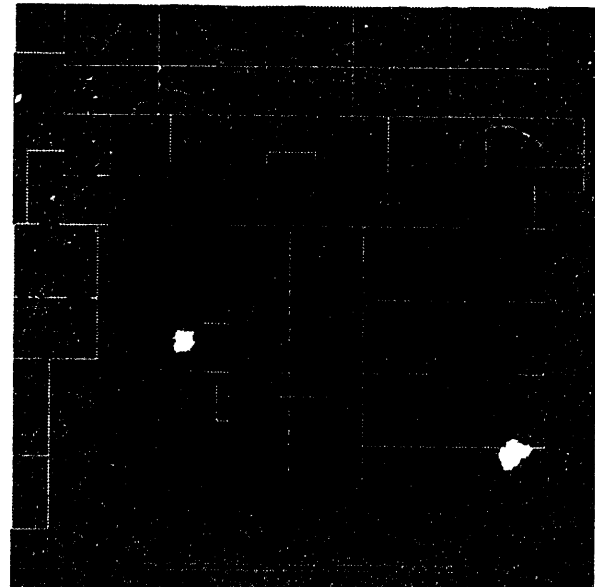


Figure 2. Density and grids at levels 1 and 2.

**DATE  
FILMED**

**10/20/94**

**END**

